



ORIGINAL RESEARCH ARTICLE

# Synthesis and Microwave Dielectric Properties of BBSZ-Zinc Silicate Based Material for LTCC Applications

RAVINDRA DESHMUKH,<sup>1</sup> VARSHA CHAWARE,<sup>1</sup> R. RATHEESH,<sup>2</sup>  
and GIRISH J. PHATAK<sup>1,3</sup> 

1.—Centre for Materials for Electronics Technology (C-MET), Pune 411008, India. 2.—Centre for Materials for Electronics Technology (C-MET), Hyderabad, Telangana 500051, India. 3.—e-mail: gjp@cmet.gov.in

The microwave dielectric properties and microstructures of zinc silicate ( $\text{Zn}_2\text{SiO}_4$ ) ceramic with the addition of 5–20 wt.%  $\text{B}_2\text{O}_3\text{-Bi}_2\text{O}_3\text{-SiO}_2\text{-ZnO}$  (BBSZ) glass have been studied for low-temperature co-fired ceramic (LTCC) applications. BBSZ glass helps in reducing the sintering temperature of zinc silicate (ZS) from about 1350°C to around 900°C in the form of ZS-glass composites. The zinc silicate powder was prepared following solid-state reaction technique, while BBSZ glass was prepared by standard melting and quenching method. Expectedly, the sintering studies indicate increasing sintered density between 91% and 97% with increasing sintering temperature from 875°C to 950°C. The sintering density is also seen to increase with increasing content of BBSZ, indicating liquid-phase sintering of the composites. Higher glass content in the composite leads to increased dielectric constant as well as dielectric loss. The results indicate that ZS with the addition of 5 wt.% of BBSZ glass, sintered at 925°C for 3 h, exhibits good microwave dielectric properties with a dielectric constant ( $\epsilon_r$ ) of 6.5 and quality factor ( $Q \times f$ ) of 20,754 GHz, which is suitable for LTCC applications.

**Key words:** LTCC, sintering, dielectric constant, dielectric loss factor, microwave materials

## INTRODUCTION

Over the past two decades, the wireless and telecommunications industry has grown at a brisk rate. One important reason for this growth is the strides in the development of electronic materials and their related packaging technologies. Low-temperature co-fired ceramic (LTCC) technology is a key microwave circuit fabrication technology used for fabricating devices for wireless and telecommunication industries at the GHz frequency range.<sup>1</sup> Several types of microwave circuits and components have been reported in LTCC, which include radar circuits, antennas, Bluetooth modules, and front-end modules for mobile phones and wireless local

area networks.<sup>2</sup> These devices are fabricated using well-established commercial LTCC materials.<sup>1</sup> However, to cater to the ever-increasing demands of high-operating-frequency devices, multi-functionality, miniaturization together with high speeds, there is a need to focus on new LTCC materials with improved dielectric properties. Several ceramic materials are known to have very good dielectric properties, such as low dielectric constant ( $< 6$ ) and dielectric loss factor in the range of  $10^{-5}$ , such as, for example,  $(\text{Mg}_{0.9}\text{Ni}_{0.1})_2\text{Al}_4\text{Si}_5\text{O}_{18}$ ,  $\text{NaAlSi}_3\text{O}_8$ ,  $\text{Mg}_2\text{P}_2\text{O}_7$ , and  $\text{K}_{0.67}\text{Ba}_{0.33}\text{Ga}_{1.33}\text{Ge}_{2.67}\text{O}_8$ .<sup>3,4</sup> Silicate-based materials are often used as a substrate material at microwave frequency range due to their low  $\epsilon_r$  and high quality factor ( $> 10$  K). The silicates prepared by the sol-gel synthesis technique have also shown better dielectric properties.<sup>5</sup> Several silicate-based materials such as  $\text{Mg}_2\text{SiO}_4$ ,  $\text{MgSiO}_3$ ,  $\text{ZrSiO}_4$ , Cu-doped  $\text{Mg}_2\text{SiO}_4$ , and  $\text{Zn}_2\text{SiO}_4$  are well

known for substrate application at microwave frequency range.<sup>6–9</sup> However, most of these materials cannot be used for LTCC because of their high sintering temperature. There are some known strategies for reducing the sintering temperature of these materials, which include the addition of low-melting-point glasses or the addition of low-melting-point oxides, which can be employed in order to use these materials for LTCC application.<sup>10–12</sup>

Generally, zinc silicate ( $\text{Zn}_2\text{SiO}_4$ ) has shown very good dielectric properties. It possesses a low dielectric constant ( $\sim 6.1$ ) and low dielectric loss, in the range of  $10^{-5}$ .<sup>13,14</sup> However, its sintering temperature is high ( $\sim 1350^\circ\text{C}$ ), which needs to be reduced using appropriate additives for its use as LTCC host material. There are several reports for reducing the sintering temperature of zinc silicate using low-melting-point oxides and glasses, such as  $\text{B}_2\text{O}_3$ ,  $\text{Bi}_2\text{O}_3$ ,  $\text{Li}_2\text{CO}_3$ ,  $\text{ZnO-B}_2\text{O}_3\text{-SiO}_2$  (ZBS), and zinc borate-based glasses. The composites made using these sintering aids have shown excellent dielectric properties, and their suitability for reducing the sintering temperature has been shown.<sup>15–19</sup> Similarly,  $\text{B}_2\text{O}_3\text{-Bi}_2\text{O}_3\text{-SiO}_2\text{-ZnO}$  (BBSZ) glass has been reported as an effective low-temperature sintering aid and possesses acceptable microwave dielectric properties.<sup>16,20,21</sup> The BBSZ glass-based composite has also been reported as a very good microwave dielectric material for ultra-low sintering temperature applications. The BBSZ glass with 50 vol.% addition of  $\text{Al}_2\text{O}_3$  has shown a dielectric constant of 8.5 and loss tangent of 0.008 at 1-GHz frequency at a very low sintering temperature of  $\sim 650^\circ\text{C}$ .<sup>22</sup> In this report, we have used BBSZ glass to reduce the sintering temperature of zinc silicate, and its effects on the sintering behavior, phase composition, microstructure, and microwave dielectric properties of  $\text{Zn}_2\text{SiO}_4$  are discussed.

## EXPERIMENTAL

The zinc silicate ceramic was prepared by a solid-state route, while the BBSZ glass was prepared by mixing and melting of oxides, followed by quenching in water. Pure powders of  $\text{ZnO}$ ,  $\text{SiO}_2$ ,  $\text{B}_2\text{O}_3$ , and  $\text{Bi}_2\text{O}_3$  (Sigma Aldrich, purity > 99.5%) oxides were used as the raw materials. Zinc silicate ( $\text{Zn}_2\text{SiO}_4$ ) was prepared by wet mixing of stoichiometric quantities of zinc oxide ( $\text{ZnO}$ ) and silicon dioxide ( $\text{SiO}_2$ ) using a planetary mill in a zirconia jar with acetone. This milling was carried out for 6 h in a zirconia jar using zirconia balls. The slurry was then dried using an infrared (IR) lamp, and the dried powder was calcined at  $1150^\circ\text{C}$  for 3 h in air atmosphere. The BBSZ glass was prepared by mixing  $\text{B}_2\text{O}_3$ ,  $\text{Bi}_2\text{O}_3$ ,  $\text{ZnO}$ , and  $\text{SiO}_2$  in a molar ratio of 27:35:32:6, respectively. This mixture was milled using a planetary mill in acetone for 6 h in a zirconia jar with zirconia balls. This powder was dried, transferred to a platinum crucible, and kept in a muffle furnace at  $900^\circ\text{C}$  for 1 h. The

molten mix was quenched in deionized (DI) water. The quenched glass lumps were further milled in a planetary mill for 15 h. The calcined and milled zinc silicate (ZS) powder was then mixed with BBSZ glass frit in ZS-glass weight ratios of 5%, 10%, 15%, and 20%. These glass-ceramic powders were mixed with 5 wt.% of high-molecular-weight polyvinyl alcohol (PVA) (85 k to 124 k g/mole). The PVA mixed glass-ceramic powders were then uniaxially pressed using a die with a 12-mm diameter at 180–200-MPa pressure to form green pellets. The theoretical density of the green pellets was calculated using the following equation.<sup>23</sup>

$$D = \frac{w_1 + w_2}{\frac{w_1}{d_1} + \frac{w_2}{d_2}} \quad (1)$$

where  $W_1$  and  $W_2$  represent the weight of zinc silicate and BBSZ glass measured in air, respectively. Similarly,  $d_1$  and  $d_2$  are the theoretical densities of zinc silicate and BBSZ glass, respectively. Here, the density of zinc silicate was taken as 4.23 gm/cc from a previous report,<sup>14</sup> while the density of BBSZ glass, as measured using the Archimedes principle, was 6.85 gm/cc. This value of density matches with that reported in the literature.<sup>24</sup> The calculated theoretical density of the mixture was used as a reference in each case. The green pellets were sintered at temperatures between  $875^\circ\text{C}$  and  $950^\circ\text{C}$  in steps of  $25^\circ\text{C}$ . The sintering was carried out for 3 h at a heating rate of  $5^\circ\text{C}/\text{min}$  in air atmosphere.

The calcined and sintered glass-ceramic pellets were characterized for structural properties by x-ray diffraction (XRD, D8 Advance, Bruker, Germany). The XRD studies were supplemented by Raman spectroscopy (Renishaw, UK). The thermal properties of the glass were studied by thermogravimetric analysis (TGA) and differential scanning calorimetry (DSC) techniques (TA Instruments SDT Q600). The microstructure was observed by scanning electron microscopy (SEM, Hitachi S-4800). The bulk density of the pellets and glass frit lumps was measured by the Archimedes method (Mettler weighing balance, AB204-S). The microwave dielectric properties were measured by the dielectric resonator cavity method (QWED model) in  $\text{TE}_{01\delta}$  mode using a 15 GHz vector network analyzer (VNA, MS2027C, Anritsu, Japan). The dilatometric studies were carried out by preparing separate green pellets of the diameter of 6 mm and about 5-mm height, using a laboratory-made vertical dilatometer having the Z-axis measurement least count of  $1\text{ }\mu\text{m}$  in the temperature range of RT to  $1000^\circ\text{C}$ .

## RESULTS AND DISCUSSION

Figure 1 presents the XRD patterns of as-quenched BBSZ glass, zinc silicate (ZS) powder calcined at  $1150^\circ\text{C}$ , ZS ceramic with BBSZ glass pellet sintered at  $925^\circ\text{C}$ , and the standard XRD

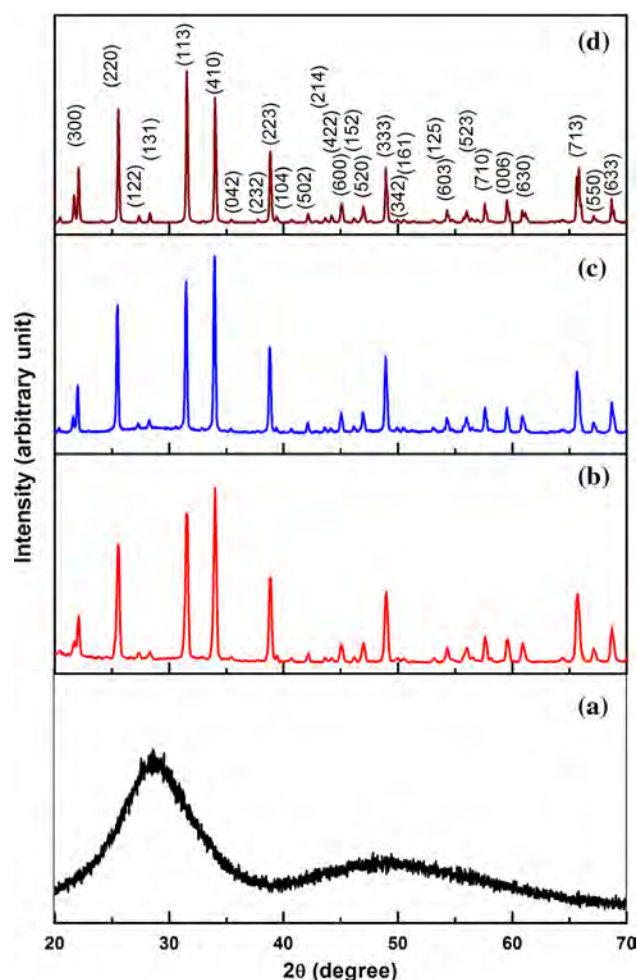


Fig. 1. The XRD patterns for (a) as-quenched BBSZ glass, (b) standard zinc silicate pattern from JCPDS card number 0-037-1485, (c) zinc silicate powder calcined at 1150°C, and (d) BBSZ glass-added zinc silicate.

pattern for ZS ceramic (JCPDS card number 0-037-1485), respectively. The XRD pattern of calcined ZS powder confirms the single-phase formation of  $\text{Zn}_2\text{SiO}_4$  after calcination. The well-diffracted peaks confirm the highly crystalline nature of zinc silicate which matches well with the standard JCPDS card number; no other secondary phases are observed. The formation of pure ZS ceramic was also confirmed by Raman spectroscopy, presented further in Fig. 2. Pure ZS formation by calcining the mixture of ZnO and  $\text{SiO}_2$  powders at 1150°C has been previously reported.<sup>14</sup> The XRD pattern of BBSZ glass powder confirms its amorphous nature. The XRD patterns of sintered zinc silicate-glass pellets confirm the absence of any chemical interaction between the glass and the ceramic phase. This ensures the unfettered contribution of ceramic material to the dielectric properties of the composite. Figure 2 presents the Raman spectra for zinc silicate, which match well with the standard available database, confirming single-phase formation of ZS.<sup>25</sup> The  $\text{Zn}_2\text{SiO}_4$  ceramic shows very strong

vibration peaks in the internal mode regions of  $\text{SiO}_4^{4-}$  tetrahedra. The characteristic bands observed in the 300–700  $\text{cm}^{-1}$  range can be assigned to bending vibrations and those in the 800–1100  $\text{cm}^{-1}$  range can be assigned to the stretching vibrations of the  $\text{SiO}_4$  tetrahedra.<sup>26</sup> In the present study, symmetric stretching vibrations of  $\text{SiO}_4$  tetrahedra are observed as a strong band at 871  $\text{cm}^{-1}$ , whereas asymmetric stretching vibrations are observed as medium-intensity bands at 908  $\text{cm}^{-1}$  and 947  $\text{cm}^{-1}$ . The symmetric and asymmetric bending modes of  $\text{SiO}_4$  tetrahedra are observed at 476  $\text{cm}^{-1}$  and 395  $\text{cm}^{-1}$ , respectively. The bands observed below 300  $\text{cm}^{-1}$  are in the lattice mode region where an unequivocal assignment of modes is not possible because of the appearance of rotational and translation modes of  $\text{SiO}_4$  tetrahedra, and other metal-oxygen vibrational modes.<sup>27</sup>

The BBSZ glass was analyzed using TGA and DSC. The weight loss and heat flow curves of BBSZ glass are presented in Fig. 3. It is seen from the heat flow curve that the first endothermic peak is observed at 385°C, which indicates the glass transition temperature ( $T_g$ ). The exothermic peak at 530°C reveals the crystallization temperature ( $T_c$ ), while the well-formed second endothermic peak at 660°C indicates the melting temperature ( $T_m$ ) of glass.<sup>20,21</sup> The TGA study shows less than 1.2% weight loss, of which maximum weight loss is observed up to 400°C, corresponding to water and carbon burn out. Practically, no glass evaporation is seen up to 1000°C.

Figure 4 presents the densification studies of pellets with various glass contents. Overall, peak densification up to 97% is seen for all ZS-glass compositions. Even at the low glass content of 5 wt.%, the density is above 91% at 875°C sintering temperature, which is seen to increase to 97% at 950°C. As glass content increases to 10% to 20%, the peak density is achieved at a relatively lower temperature. The results show a minor reduction in density by about 2% for pellets containing 20 wt.% glass at 950°C. This possibly indicates the initiation of overgrowth, causing trapped porosity. Reduction in the sintering temperature for  $\text{ZnO-xSiO}_2$  ( $x = 0.5$  to 1) ceramic due to addition of  $\text{Li}_2\text{CO}_3\text{-Bi}_2\text{O}_3$  is reported in literature.<sup>28</sup> Jia-Li Zou et al. also reported that the bulk density of the zinc silicate with  $\text{Bi}_2\text{O}_3$  samples increased with an increase in sintering temperature from 850°C to 950°C, because of densification of the microstructure and pore removal. However, a further increase in sintering temperature to 950°C results in abnormal grain growth. The abnormal grain growth causes a decrease in bulk density.<sup>29</sup> Similar observations were reported by Lv and Zuo, where the reduction in density was ascribed to grain coarsening induced by a liquid phase at higher sintering temperature.<sup>30</sup>



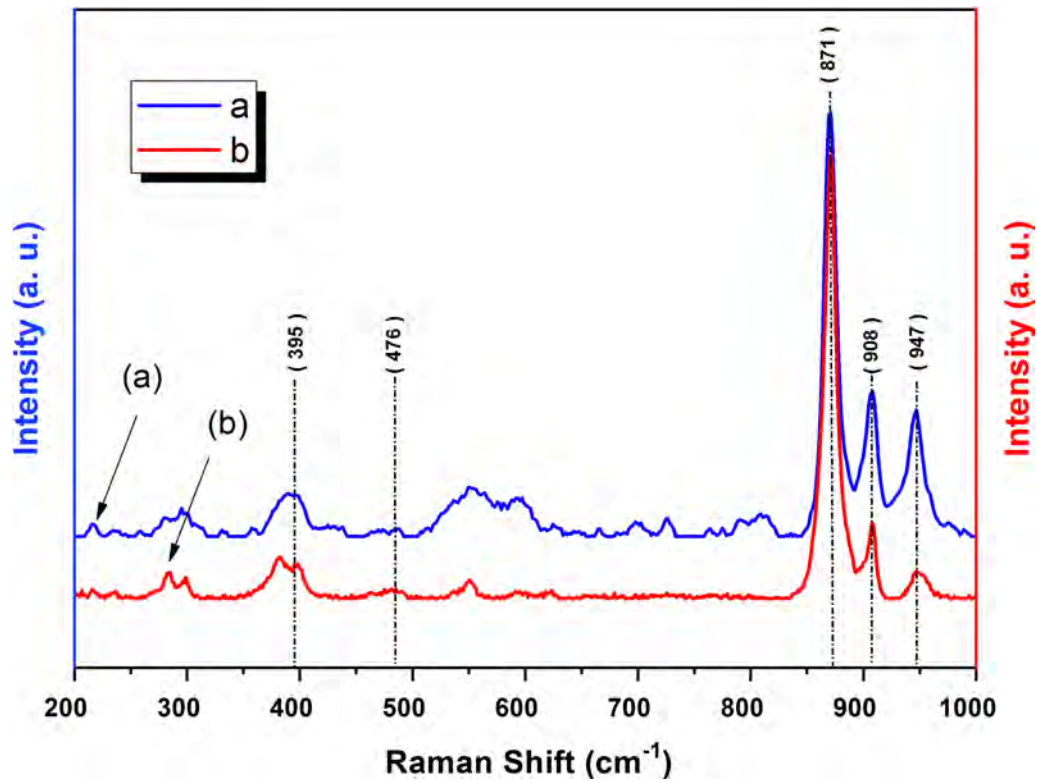


Fig. 2. Raman spectra of  $\text{Zn}_2\text{SiO}_4$ : (a) pure ZS powder prepared and calcined at  $1150^\circ\text{C}$ , and (b) from the standard  $\text{Zn}_2\text{SiO}_4$  database.

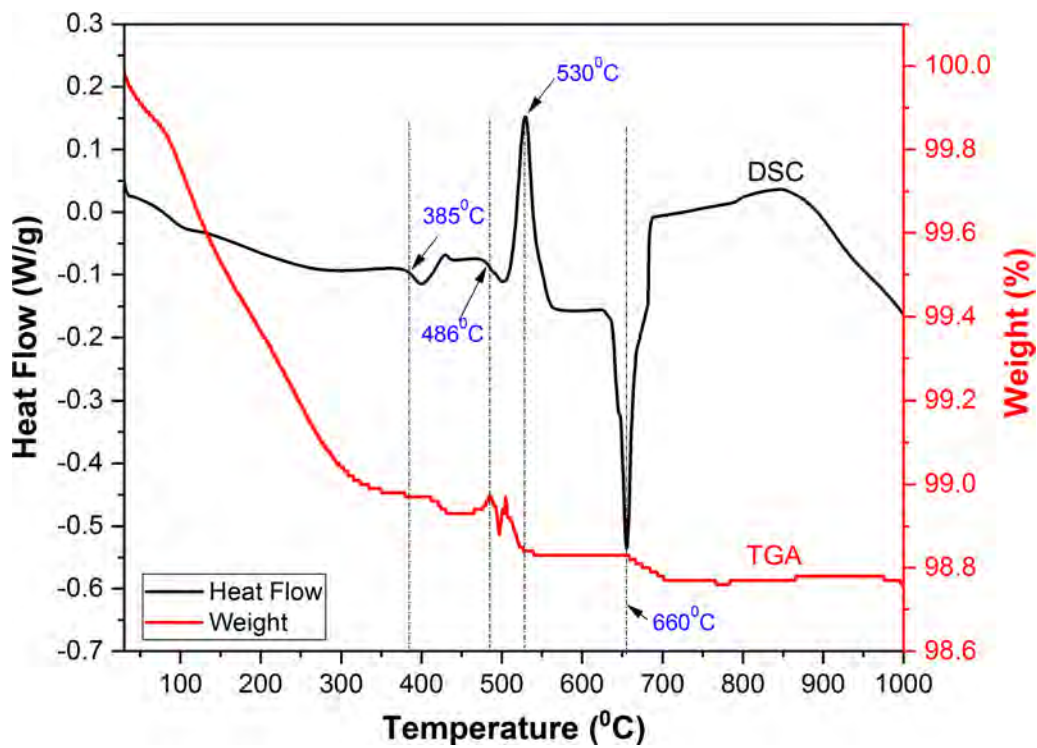


Fig. 3. TGA and DSC study for BBSZ glass.

Figure 5 shows the surface microstructures of glass-ceramic samples with 5 wt.% glass loading at different sintering temperatures from  $875^\circ\text{C}$  to

$950^\circ\text{C}$ . It is seen that all samples show a well-developed dense microstructure with a grain size of about  $1\text{--}3\ \mu\text{m}$ . Generally, grain growth is expected

with increasing sintering temperature. While there is a hint of grain growth with increasing temperature, these pictures do not conclusively indicate the same. The improved density with temperature, however, indicates liquid-phase sintering due to molten BBSZ glass, as the melting temperature of

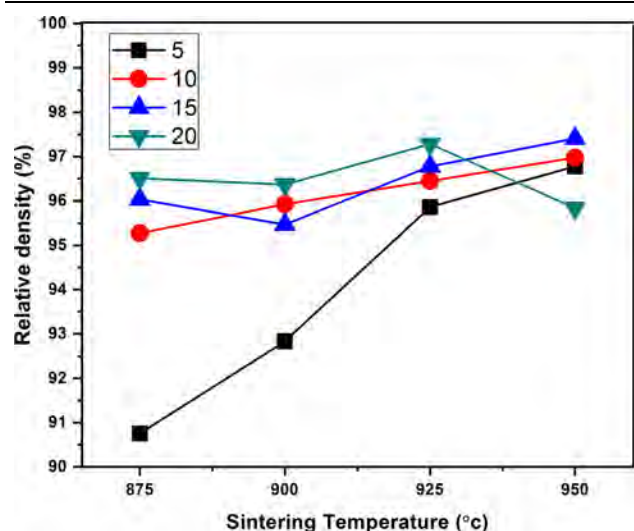


Fig. 4. Densification study for zinc silicate pellets with BBSZ glass.

the BBSZ glass is about 660°C. This can be seen from the heat flow curve of the BBSZ glass presented in Fig. 3.

Figure 6 presents the dilatometer curves for pellets with 5 wt.%, 10 wt.%, 15 wt.%, and 20 wt.% BBSZ glass containing pellets along with the temperature differential of  $\Delta L/L_0$ , where  $L_0$  is the original length, and  $\Delta L$  is change in length.<sup>31</sup> The lowering of sintering temperature with increasing glass content indicates liquid-phase sintering. Evidence of liquid-phase sintering assisting in the reduction in sintering temperature has also been presented by Kim et al. for the sintering of  $\text{BaTi}_4\text{O}_9$  pellets using zinc borate glass.<sup>32</sup> Lu et al. have reported that the addition of BBSZ glass into ZnO-based ceramic improved the densification at much lower sintering temperature.<sup>33</sup> It is reported for BBSZ-assisted sintering of *M*-type barium ferrite  $[\text{Ba}(\text{CoTi})_{1.5}\text{Fe}_9\text{O}_{19}]$  that liquid-phase BBSZ glass promoted grain growth.<sup>33</sup> Liquid-phase sintering is well reported in the literature. During sintering, the molten liquid phase wets and flows between the grains, causing their rearrangement. In many cases, such as reported by Wang et al.,<sup>34</sup> the dissolution of grains into liquid causes transportation and grain coarsening.<sup>35</sup> In the present case, however, while there is good evidence of liquid-

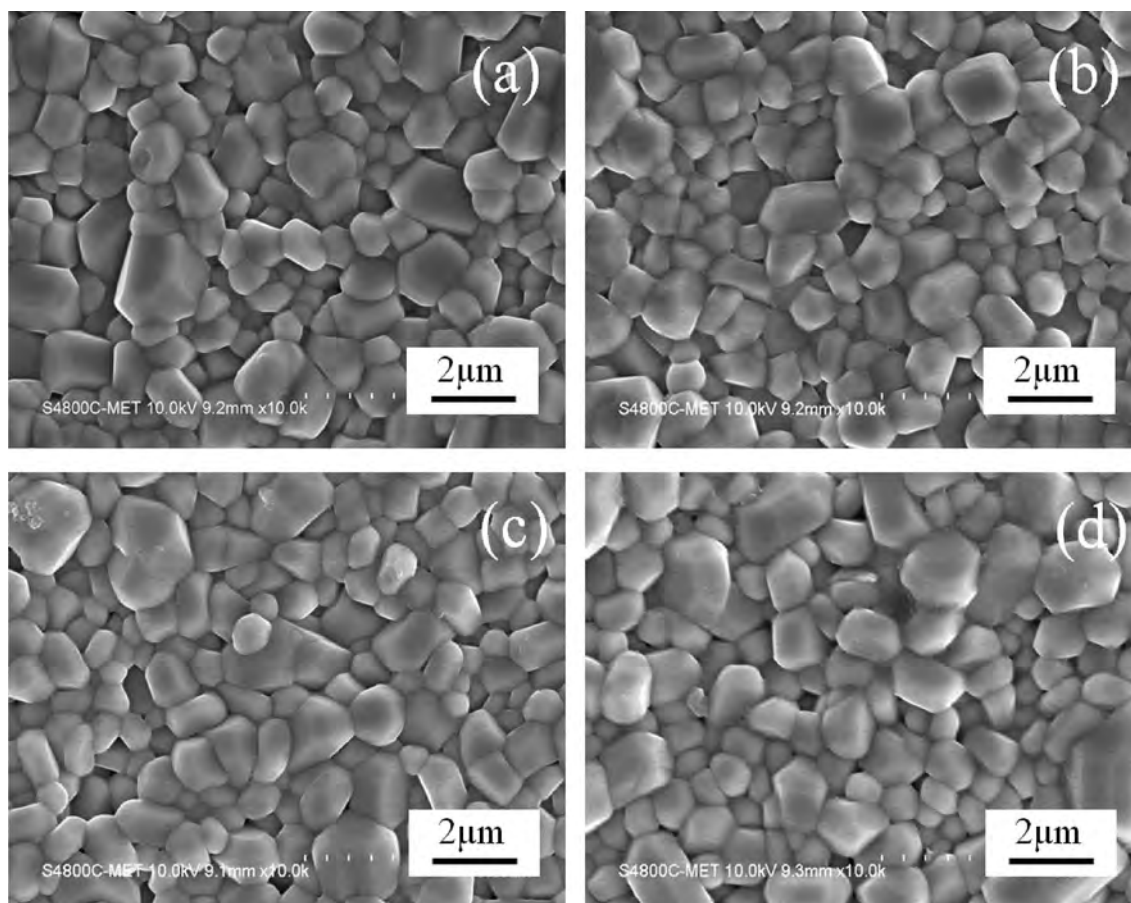


Fig. 5. Micrographs of ceramic samples with 5 wt.% BBSZ loading in ZS sintered at (a) 875°C, (b) 900°C, (c) 925°C, and (d) 950°C.

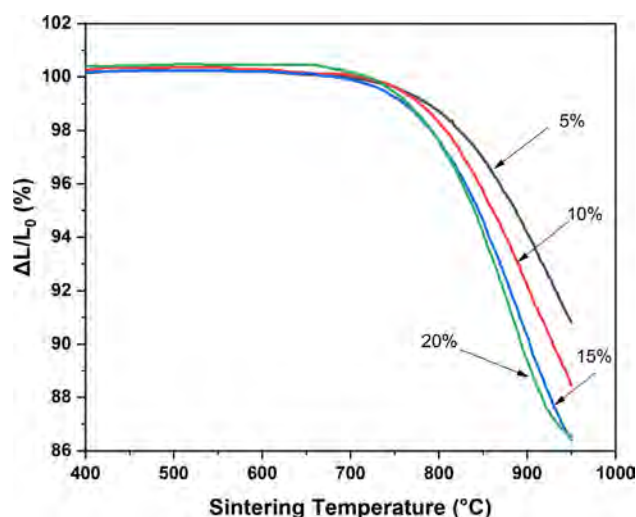


Fig. 6. Dilatometer study for ZS + BBSZ pellets with 5 wt.%, 10 wt.%, 15 wt.%, and 20 wt.% BBSZ glass.

assisted sintering from the dilatometer studies presented above, the lack of considerable grain growth at higher sintering temperature points towards the possibility of limited dissolution and transportation through the liquid phase. It is reported that if there is no dissolution of solid into the liquid, the densification occurs at the rate of densification of solid alone, and the liquid is simply a pore-filling agent.<sup>27</sup>

Figure 7 presents the dielectric properties, namely dielectric constant and quality factor ( $Q \times f$ ), of the samples. Generally, the dielectric constant is seen to follow the density curves for all individual samples. That is, the dielectric constant increases as the density of the sample improves. This behavior of sintered samples is expected, as a reduction in porosity will improve the dielectric constant. Such behavior has been reported previously for ceramic with added glass.<sup>20,36</sup> Further, it can be seen that the dielectric constant of the composites increases from 6.5 to 8.5 with increasing content of the glass. It is known that the addition of bismuth-based glass increases the dielectric constant of glass-ceramic due to an increase in polarization.<sup>37</sup> A similar trend is seen in the present study.

While the addition of glass causes an increase in the dielectric constant due to bismuth content, the dielectric loss is also seen to increase as the glass content increases.<sup>11</sup> The dielectric loss is governed by the intrinsic and extrinsic properties of the material. The presence of amorphous material in the form of glass causes an increase in the dielectric loss. The present results show that the addition of glass at 10 wt.% or higher causes a drastic reduction in quality factor. The samples with 5 wt.%, therefore, show the highest values of  $Q \times f$ , which is above 20,700 GHz when sintered at 900°C or above. The dense microstructure and low amorphous contents might have helped in achieving the highest

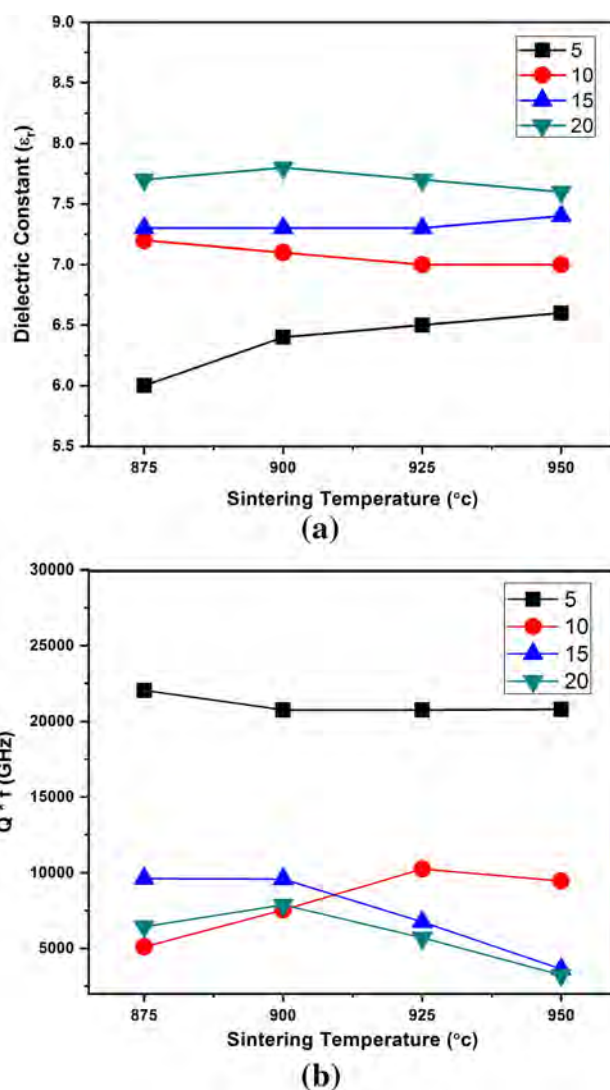


Fig. 7. Dielectric properties of zinc silicate pellets with addition of BBSZ glass from 5 wt.% to 20 wt.%. (a) Dielectric constant and (b) quality factor ( $Q \times f$ ).

value of quality factor for a 5 wt.% glass-ceramic sample. These results are comparable to the glass containing zinc silicate-based ceramic reported in the literature. The best microwave dielectric properties have been reported for  $B_2O_3$  added in  $Zn_2SiO_4$  ceramic sintered at 900°C for 2 h, which shows  $Q \times f$  of 70,000 GHz and dielectric constant of 6.<sup>37</sup> Another report of the addition of  $Bi_2O_3$  to  $Zn_2SiO_4$  sintered at 885°C for 2 h also reports dielectric properties, which are  $Q \times f$  of 12,600 GHz with a dielectric constant of 7.<sup>36</sup> While the above report indicates that good dielectric properties have been achieved for ZS ceramic with the addition of  $B_2O_3$ , it is reported that  $B_2O_3$  does affect the tape-casting process, as it reacts with the organics used in the tape-casting process and affects the viscosity of the slurry. Further, it is reported that the addition of  $Bi_2O_3$  forms a secondary phase at a sintering temperature of about 900°C which results in a high dielectric constant of about 10.<sup>38</sup> Other literature



indicates that the  $V_2O_5$ -based sintering aid does help in reducing the sintering temperature of zinc silicate to  $875^\circ\text{C}$ . However, the  $V_2O_5$  sintering aid reacts with silver, making it difficult for use in LTCC.<sup>39</sup> The addition of ZBS glass to zinc silicate also reduces the sintering temperature to  $900^\circ\text{C}$ .<sup>40</sup> This material showed a dielectric constant of 6.85 and  $Q \times f$  of 31,690 GHz. It is seen that the present results are comparable to other ZS composites. Moreover, the choice of BBSZ glass as a sintering aid for ZS avoids difficulties related to tape casting, and is known to be non-reactive with silver.<sup>41–43</sup> Similarly, ZS is also reported to be non-reactive with silver.<sup>14</sup> Our studies based upon XRD spectra indicate that for co-sintering of silver with the ZS-BBSZ composite at  $925^\circ\text{C}$ , no chemical reaction of silver occurs during sintering.

Considering that the 5 wt.% BBSZ-containing samples sintered at  $950^\circ\text{C}$  have the highest density and best quality factor, they are best suited for microwave applications. However, this sintering temperature is quite close to the melting temperature of silver and may cause a narrow process window for LTCC. On the other hand, the sample sintered at  $925^\circ\text{C}$  has only about 2% lower density and almost equal quality factor. Therefore, the  $925^\circ\text{C}$ -sintered, 5 wt.% glass-containing samples showing a dielectric constant ( $\epsilon_r$ ) of 6.5 and quality factor ( $Q \times f$ ) of 20,754 GHz seem best suited for LTCC applications.

## CONCLUSIONS

Zinc silicate ceramic was prepared by a solid-state ceramic route for LTCC applications. The bismuth-based BBSZ glass was added to lower the sintering temperature of zinc silicate. Sintering studies between  $875^\circ\text{C}$  and  $950^\circ\text{C}$  for various ZS-BBSZ composites with BBSZ content varying between 5 wt.% and 20 wt.% indicate relative density of more than 91% at sintering temperatures of  $900^\circ\text{C}$  and above. Higher glass content and higher sintering temperature improve the sintering density, but the amorphous phase of glass causes a reduction in quality factor. The sintering study based upon density measurements and dilatometer studies as well as the microstructure evolution with temperature evidently indicate liquid-phase sintering of the samples with the limited dissolution of ceramic in the liquid phase. The zinc silicate powder mixed with 5 wt.% BBSZ glass and sintered at  $925^\circ\text{C}$  has shown a very good quality factor ( $Q \times f$ ) of 20,754 GHz and a low dielectric constant ( $\epsilon_r$ ) of 6.5, which may be suitable for LTCC substrate applications.

## ACKNOWLEDGMENTS

Author Ravindra Deshmukh is grateful to the Department of Science and Technology (DST) and Centre for Materials for Electronics Technology (CMET), Pune, for financial assistance and support.

## CONFLICT OF INTEREST

The authors declare that they have no conflict of interest.

## REFERENCES

1. R. Ghaffarian, *Facta Univ. Electron. Energy Ser. Electron. Energ.* 29, 543 (2016). <https://doi.org/10.2298/fuee1604543g>.
2. L.K. Yeung, J. Wang, Y. Huang, S.-C. Lee, and K.-L. Wu, in *2005 Asia-Pacific Microwave Conference Proceedings* (IEEE, Suzhou, China, 2005), pp. 1–4.
3. M.T. Sebastian, R. Uvic, and H. Jantunen, *Int. Mater. Rev.* 60, 392 (2015).
4. M.T. Sebastian, *Dielectric Materials for Wireless Communication* (Amsterdam: Elsevier, 2008).
5. J. Varghese, T. Joseph, and M. T. Sebastian, in *AIP Conference Proceedings* (2011), pp. 193–197.
6. H. Ohsato, J. Varghese, and H. Jantunen, *Dielectric Losses of Microwave Ceramics Based on Crystal Structure, Electromagnetic Materials, and Devices*, eBook (PDF) ISBN: 978-1-83880-102-1 (2020).
7. J. Varghese, N. Joseph, H. Jantunen, S.K. Behera, H.T. Kim, and M.T. Sebastian, *Microwave Materials for Defense and Aerospace Applications, Handbook of Advanced Ceramics and Composites* (Berlin: Springer, 2019).
8. H. Ohsato, J. Varghese, T. Vahera, J. Seog Kim, M.T. Sebastian, H. Jantunen, and M. Iwata, *J. Korean Ceram. Soc.* 56, 526 (2019).
9. J. Varghese, T. Joseph, and M.T. Sebastian, *Mater. Lett.* 65, 1092 (2005).
10. M.T. Sebastian, R. Uvic, and H. Jantunen, *Microwave Materials*, Vol. I (Hoboken: Wiley, 2017), pp. 267–280.
11. W. Ling, H. Zhang, Y. Li, D. Chen, Q. Wen, and J. Shen, *J. Appl. Phys.* 107, 09D911 (2010).
12. I. Alibe, K. Matori, H. Sidek, Y. Yaakob, U. Rashid, A. Alibe, M. Mohd Zaid, and M. Ahmad Khiri, *Molecules* 23, 873 (2018). <https://doi.org/10.3390/molecules23040000>.
13. N.-H. Nguyen, J.-B. Lim, S. Nahm, J.-H. Paik, and J.-H. Kim, *J. Am. Ceram. Soc.* 90, 3127 (2007).
14. V. Chaware, R. Deshmukh, C. Sarode, S. Gokhale, and G. Phatak, *J. Electron. Mater.* 44, 2312 (2015).
15. G. Gao, L. Hu, H. Fan, G. Wang, K. Li, S. Feng, S. Fan, and H. Chen, *Opt. Mater.* 32, 159 (2009).
16. C. Liu, H. Zhang, H. Su, T. Zhou, J. Li, X. Chen, W. Miao, L. Xie, and L. Jia, *J. Alloys Compd.* 646, 1139 (2015).
17. B. Mohammed, M.S. Jaafar, and H. Wagiran, *J. Lumin.* 190, 228 (2017).
18. J. Kim, N. Nguyen, J. Lim, D. Paik, S. Nahm, J. Paik, J.-H. Kim, and H. Lee, *J. Am. Ceram. Soc.* 91, 671 (2008).
19. Y. Dai, Y. Sun, and W. Chen, *Adv. Mater. Res.* 66, 104 (2009).
20. I.J. Induja, P. Abhilash, S. Arun, K.P. Surendran, and M.T. Sebastian, *Ceram. Int.* 41, 13572 (2015).
21. T. Joseph, M.T. Sebastian, H. Sreemoolanadhan, and V.K. Sree Nageswari, *Int. J. Appl. Ceram. Technol.* 7, E98 (2009).
22. M.-Y. Chen, J. Juuti, C.-S. Hsi, C.-T. Chia, and H. Jantunen, *J. Am. Ceram. Soc.* 98, 1133 (2015).
23. S.N. Renjini, S. Thomas, M.T. Sebastian, S.R. Kiran, and V.R.K. Murthy, *Int. J. Appl. Ceram. Technol.* 6, 286 (2009).
24. M.-Y. Chen, 66, (IOP Publishing jultika, 2017) <http://jultika.oulu.fi/files/isbn9789526215600.pdf>. Accessed: 24 Dec 2019. <https://rruff.info/Willemite>. Accessed: 12 Jan 2020.
25. B.C. Babu, K.N. Kumar, B.H. Rudramadevi, and S. Buddhudu, *Ferroelectr. Lett. Sect.* 41, 28 (2014).
26. B. C. Babu, B. V. Rao, G. B. Kumar, G. Hungerford, N. S. Hussain, and A. Stamboulis in *Advanced Materials and Their Applications—Micro to Nano Scale*, book chapter, (Springer, 2008), pp. 194–218.
27. J.-S. Kim, N.-H. Nguyen, M.-E. Song, J.-B. Lim, D.-S. Paik, S. Nahm, J.-H. Paik, B.-H. Choi, and S.-J. Yu, *Int. J. Appl. Ceram. Technol.* 6, 581 (2009).
28. J.-L. Zou, Q.-L. Zhang, H. Yang, and H.-P. Sun, *Jpn. J. Appl. Phys.* 45, 4143 (2006).

30. Y. Lv and R. Zuo, *Ceram. Int.* 39, 2545 (2013).
31. J. Zygmuntowicz, M. Piątek, A. Miazga, K. Konopka, and W. Kaszuwara, *Process. Appl. Ceram.* 12, 111 (2018).
32. D.-W. Kim, D.-G. Lee, and K.S. Hong, *Mater. Res. Bull.* 36, 585 (2001).
33. Y. Lu, Y. Li, R. Peng, H. Su, Z. Tao, M. Chen, and D. Chen, *Appl. Ceram. Technol.* 1–6 (2019).
34. Y. Wang, Y. Liu, J. Li, Q. Liu, H. Zhang, and V.G. Harris, *AIP Adv.* 6, 056410 (2016).
35. R.M. German, P. Suri, and S.J. Park, *J. Mater. Sci.* 44, 1 (2009).
36. M.-Y. Chen, T. Vahera, C.-S. Hsi, M. Sobocinski, M. Teirikangas, J. Peräntie, J. Juuti, and H. Jantunen, *J. Am. Ceram. Soc.* 100, 1257 (2017).
37. J.-S. Kim, M.-E. Song, M.-R. Joung, J.-H. Choi, S. Nahm, S.-I. Gu, J.-H. Paik, and B.-H. Choi, *J. Eur. Ceram. Soc.* 30, 375 (2010).
38. Q.L. Zhang, H. Yang, J.L. Zou, and H.P. Wang, *Mater. Lett.* 59, 880 (2005).
39. H.C. Ling, M.F. Yan, and W.W. Rhodes, *J. Mater. Res.* 5, 1752 (1990).
40. K. Tang, Q. Wu, and X. Xiang, *J. Mater. Sci. Mater. Electron.* 23, 1099 (2012).
41. R. Karmazin, O. Dernovsek, N. Ilkov, W. Wersing, A. Roosen, and M. Hagymasi, *J. Eur. Ceram. Soc.* 25, 2029 (2005).
42. P.S. Anjana, M.T. Sebastian, and J. Am, *Ceram. Soc.* 92, 96 (2009).
43. S. Thomas and M.T. Sebastian, *Mater. Res. Bull.* 43, 843 (2008).

**Publisher's Note** Springer Nature remains neutral with regard to jurisdictional claims in published maps and institutional affiliations.